Earth Reinforcement, Ochiai, Yasufuku & Omine (eds)© 1996 Balkema, Rotterdam. ISBN 90 5410 8339

Instability patterns of reinforced-soil structures

R. L. Michalowski
The Johns Hopkins University, Baltimore, Md, USA

ABSTRACT: It is an accepted practice in the design of reinforced-soil structures to use a perfectly-plastic material model to simulate the behavior of the granular fill. An approach based on limit analysis theorems is then applicable, where the factor of safety, critical height of a slope, or the necessary amount of reinforcement, can be estimated. Application of limit analysis to reinforced slopes is presented.

1 INTRODUCTION

Stability of soil-reinforced structures is commonly analyzed using a limit-equilibrium technique. An alternative method is that based on the kinematical theorem of limit analysis. Both techniques use a perfectly-plastic model for both the structure's fill and reinforcement, and assume that the soil deformation conforms to the normality rule (associative flow), although the limit equilibrium technique does not make this assumption explicitly.

The limit analysis approach is preferred here, since it requires explicitly construction of a kinematically admissible mechanism, and it leads to a strict upper bound to the critical height or a limit load, or to the lower bound on the amount of reinforcement necessary to avoid collapse. The two techniques, however, will provide the same answer if calculations are based on identical failure mechanisms, and the limit equilibrium calculations are carried out consistently.

The method used here is presented briefly, and its application to a rotational failure is shown. Some peculiarities in the collapse pattern are indicated, which relate to possible kinking of the reinforcement and pull-out of reinforcement layers which are not necessarily the most upper layers in the structure.

2 REINFORCED SLOPES

The structures considered here are slopes built over foundation soils with the same properties as the slope fill. Mechanisms with failure surfaces extending into the foundation are permitted. The strength of soil is described by the standard Mohr-Coulomb failure criterion with no cohesion. The plastic deformation of soil is assumed to be governed by the normality rule. The yielding force in a single layer of reinforcement is characterized by its tensile strength per unit width, T_t. The influence of confining stress on the strength of the reinforcement is neglected. Only the primary reinforcement is considered. It is convenient to introduce an average reinforcement strength k_t defined as

$$k_t = \frac{n T_t}{H} \qquad (1)$$

where n is the number of reinforcement layers, and H is the slope height. If reinforcement consists of separate strips (rather than grids), T_t needs to be taken as the strength of a single strip times the number of strips per unit width of the structure (number of strips per unit width need not be an integer).

The amount of primary reinforcement necessary to prevent collapse of a slope of a given height, H, can be expressed as a dimensionless quantity, $k_t/\gamma H$, where γ is the unit weight of the soil. The problem can be formulated then to solve for $k_t/\gamma H$. Alternatively, one can present results as a normalized critical height, $\gamma H/k_t$, of a slope with a given average reinforcement strength k_t.

The objective of this paper is not to produce design charts, but to indicate collapse patterns which are usually not anticipated.

3 ANALYSIS TECHNIQUE

The kinematical theorem of limit analysis is used here. This theorem states that *the rate of work done by traction and distributed forces is less than or*

equal to the energy dissipation in any kinematically admissible failure mechanism

$$\int_V \sigma_{ij}^* \dot{e}_{ij}^* dV \geq \int_S T_i v_i dS + \int_V X_i v_i^* dV \qquad (2)$$

where $\dot{e}_{ij}^*$ is the strain rate in a kinematically admissible velocity field, σ_{ij}^* is the stress tensor associated with $\dot{e}_{ij}^*$, velocity $v_i^* = v_i$ on boundary S (a given kinematical boundary condition), X_i is the vector of body forces (*e.g.*, the weight), and S and V are the loaded boundary and the volume, respectively.

A kinematically admissible mechanism here is one where the kinematical boundary conditions are satisfied and the deformation of the material conforms to the associative flow rule.

Application of the theorem in eq. (2) to a slope will yield the upper bound to the limit load on the slope crest or, when $T_i = 0$, it can be used to calculate the maximum height up to which a stable slope can be built (critical height). Alternatively, the reinforced slope problem can be calculated to yield the lower bound to the strength of reinforcement necessary to prevent collapse of a slope with a given height.

4 EFFECT OF PORE WATER PRESSURE

The pore water pressure can be included in the limit analysis through including an additional term on the right-hand side of inequality (2), which represents the work of the pore water pressure on the skeleton expansion

$$W_w = -\int_V u \dot{e}_{ii}^* dV \qquad (3)$$

Compression is taken here as positive, and the minus sign indicates that positive (compressive) pore pressure u does positive work on the skeleton expansion (negative strain-rate). Pore pressure is considered here as an external force, and the failure process is considered to be drained (for details see Michalowski, 1994).

5 COLLAPSE MECHANISM

For the sake of presentation all results will be given as critical height of slopes, represented in a dimensionless fashion as $\gamma H/k_t$. A reciprocal of $\gamma H/k_t$ may be interpreted as a normalized amount of minimum reinforcement required, for a slope of a given height, to avoid collapse.

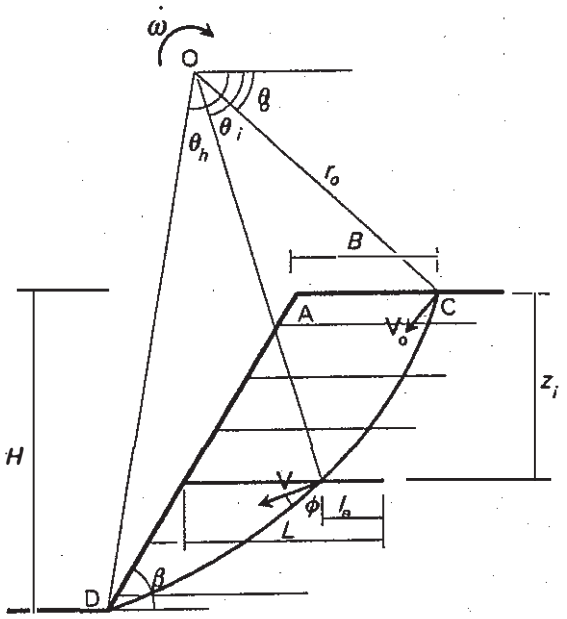

Fig. 1. Rotational collapse mechanism of a slope

The collapse mechanism considered here is comprised of a rotating block, Fig. 1, separated from the material at rest by a failure surface (CD), which, in terms of limit analysis, is interpreted as a velocity discontinuity surface. The dissipation of work occurs during incipient collapse (initial plastic flow) only along the discontinuity surface, but it may occur in both the soil (if cohesive) and in the reinforcement.

Upon incipient failure, block ACD rotates about point O, with a rotational velocity $\dot{\omega}$. The consequence of the associative flow rule is that the velocity discontinuity vectors must be inclined to the discontinuity surface at angle φ. It can be proved that for the rigid-rotation mechanism to be kinematically admissible, the shape of the failure surface CD must be a log-spiral, and the velocity must propagate along CD according to an exponential law.

5.1 *Work dissipation rate during incipient failure*

It can be shown easily that for a granular (cohesionless) soil the traction vector on the failure surface CD and the velocity jump vector are orthogonal, thus, the energy dissipation rate in the soil during the incipient collapse process is zero. The energy dissipation rate due to tensile rupture of the reinforcement can be obtained in a closed form as

$$\dot{D} = \frac{1}{2} k_t \dot{\omega} r_0^2 \left(\sin^2\theta_h e^{2(\theta_h - \theta_0)\tan\varphi} - \sin^2\theta_0\right) \qquad (4)$$

where k_t is given in eq. (1), and all other symbols are explained in Fig. 1. The work dissipation rate in eq. (4) is, in this boundary value problem, equal to the left-hand side of inequality (2). There is no load on the top surface of the slope, therefore the first term on the right-hand side is equal to zero. The second term on the right-hand side of (2) represents the work rate of the soil weight, and it is a linear function of order one of γH. Consequently, an upper bound to $\gamma H/k_t$ can be calculated from inequality (2). The best estimate of $\gamma H/k_t$ can be made using an optimization procedure where the geometry of the mechanism in Fig. 1 is changed so that the minimum of $\gamma H/k_t$ is obtained. The shape of the failure surface that passes through the toe is a function of two independent parameters. Here, angles θ_0 and θ_h were selected.

5.2 *Pull-out mode*

If a reinforcement layer is not long enough, the failure may occur as a pull-out rather than tensile rupture. The pull-out force of an individual layer is estimated as

$$T_p = 2\gamma z^*(1 - r_u)\, l_e\, \mu_b \qquad (5)$$

where $\gamma z^*(1 - r_u)$ is the overburden pressure, l_e is the effective length, μ_b is the friction coefficient between the soil and reinforcement, and r_u is the pore water pressure coefficient. For gentle slopes overburden depth z^* may be less than the depth of reinforcement below the slope crest z. If T_p from eq. (5) is less than T_t in (1), the pull-out force should be used in calculations of the work dissipation rate. This, however, introduces some complexity into the solution procedure, since T_p is not uniform through all the layers, and it depends on the geometry of the collapse mechanism (*i.e.*, eq. (4) can no longer be used to calculate the work dissipation rate if any of the reinforcement layers fails in the pull-out regime).

The work dissipation rate due to pull-out of a single layer during the incipient collapse can be calculated from the following expression

$$\dot{D} = 2\gamma z^* r_0 \omega\, e^{(\theta - \theta_0)\tan\varphi}(1 - r_u)\, l_e\, \mu_b \sin\theta \qquad (6)$$

and the total work dissipation rate is the integral (sum) over all the layers. The details of the solution are omitted here, and attention is brought to some peculiarities in the failure mechanism for shallow slopes and steep slopes with substantial pore pressures.

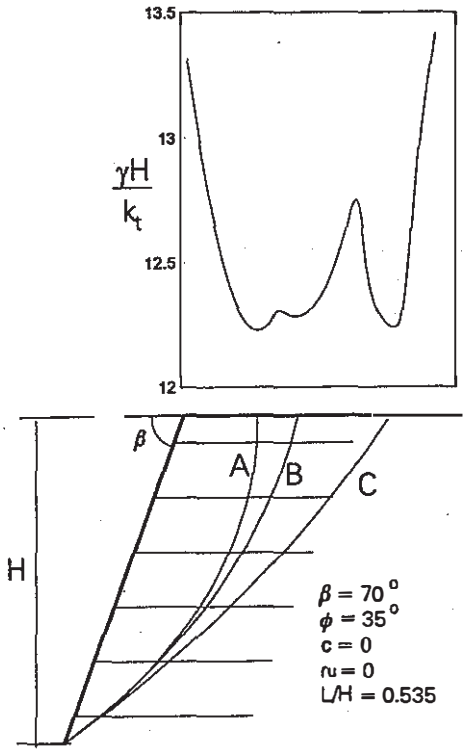

Fig. 2. Critical failure surfaces for a reinforced slope.

5.3 *Search for the minimum length of reinforcement*

Two often-considered failure modes that are directly related to the reinforcement length are: rotational or translational failure with reinforcement rupture/pull-out, and direct sliding over one layer of reinforcement. We will concentrate here only on the former.

An example of calculations is illustrated in Fig. 2. Six layers of reinforcement are used with (normalized) length of $L/H = 0.535$, and $\mu_b = 0.5$. All layers have equal strength, thus the limit reinforcement force is distributed uniformly through the slope (the critical height calculated here will then be different from that using the charts of Jewell, 1990, or Leshchinsky and Boedecker, 1989, since these charts assume a triangular distribution of reinforcement force).

If very long reinforcement is considered, the slope failure (if built to the critical height) is likely to be associated with the reinforcement rupture. Failure surface A in Fig. 2 is affiliated with the rupture of all reinforcement layers. This surface was obtained through an optimization procedure where the best upper bound (minimum) to the critical height was sought. For the given slope, the (dimensionless)

critical height, $\gamma H/k_t$, was found to be equal to 12.23.

Variation of $\gamma H/k_t$ with changes in the geometry of the failure surface is shown on the plot in Fig. 2 directly above the slope. The magnitude of $\gamma H/k_t$ is correlated to the intersection point of the failure surface with the slope crest. Distance B/H (see Fig. 1 for B) was fixed in the calculations, and $\gamma H/k_t$ was obtained for a single value of B/H from an optimization procedure where only one parameter (θ_0) was varied. Calculations were repeated for the range of B/H shown in Fig. 2.

Once the failure surface is forced to move away from its most adverse location A (associated with tensile rupture in all reinforcement layers), the upper bound to $\gamma H/k_t$ becomes higher. However, shortly before reaching position B, the pull-out force in the most upper layer of reinforcement drops below its tensile strength, which is manifested by a local minimum directly above surface B.

The variation in $\gamma H/k_t$ is due to two competing effects: a stabilizing effect of the soil weight due to removing the failure surface from its most detrimental position, and an adverse effect due to a drop in the limit force in some reinforcement layers (from their tensile strength to the pull-out force). The contribution of the remaining layers, failing in tension, of course changes also with the variation in the failure surface geometry.

For the reinforcement length selected (L/H = 0.535), $\gamma H/k_t$ increases significantly to reach a local maximum somewhere between surfaces B and C, and the critical height reaches yet another minimum at location C. An economical design of reinforcement requires that the minimum at location C has the same magnitude as that at A, *i.e.*, failure surfaces A and C are the two equally least favorable of all surfaces. Further increase in the length of reinforcement will not increase the safety of the slope, since it would only raise the second minimum. Reduction in length, however, would cause a reduction in safety since the second minimum would drop.

The necessity of simultaneously including both the tensile rupture and pull-out modes in stability analyses, as illustrated in Fig. 2, is not always recognized (although it was earlier alluded to by Jewell, 1990).

6 PECULIARITIES IN FAILURE MECHANISMS

A rational analysis of stability of slopes needs to include optimization of the collapse mechanism so that the best bound to the critical height can be found. Two examples are presented here with mechanisms which could not be anticipated easily without the optimization procedure.

A 70-degree slope with 6 layers of primary reinforcement is shown in Fig. 3. The pore water pressure is described by coefficient $r_u = 0.25$, the length of all reinforcement layers is 0.9 of the slope's height (L/H = 0.9), and the coefficient of friction between the soil and reinforcement is $\mu_b = 0.5$. The two most adverse rotational mechanisms are depicted in Fig. 3. It is clear from this example that the top layer of the (flexible) reinforcement does not contribute to the stability of the slope. For failure surface A this layer is in the compressive regime, and it would kink during collapse. The least upper bound to the critical height of this slope (associated with failure surface A) is $\gamma H/k_t$ = 4.89. The failure surface related to the second minimum ($\gamma H/k_t$ = 4.92) is denoted as B in Fig. 3. The length of the reinforcement was selected purposely here so that the two minima are approximately equal. The failure surface in the second mechanism does not intersect the top layer. The second top layer contributes a negligible pull-out force, the pull-out force in the third one is more significant, and the three bottom layers contribute in a tensile rupture regime.

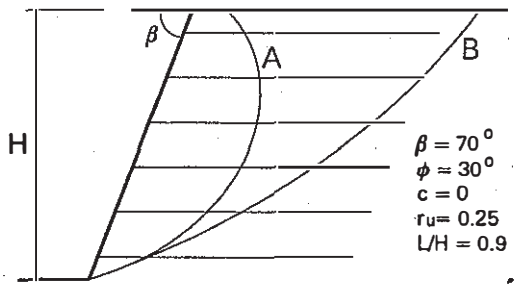

Fig. 3. Critical failure surfaces for a slope subjected to pore water pressure.

The likelihood of reinforcement kinking is not routinely considered in design, and it is clear from this example that it can have a detrimental effect on reinforced slopes when pore water pressure is involved.

The second example is presented in Fig. 4. All reinforcement layers are, again, of the same length, have the same tensile strength, and $\mu_b = 0.5$. One usually expects that, if a top layer of reinforcement is not pulled out, then the subsequent layers will also fail in a tensile rupture regime. There may be cases where it is not necessarily so, particularly for slopes with a gentle angle of inclination. Failure surface A in Fig. 4 involves rupture of all reinforcement layers, and the critical height calculated is $\gamma H/k_t$ = 36.79. The length of reinforcement was selected such that the failure along surface B yields almost the same

critical height ($\gamma H/k_t$ = 37.18). Failure along B, however, involves rupture of the two top layers, pull-out of the third one, surface B bypasses the fourth layer, and the bottom two layers would fail in the tensile regime. The critical height (or the required amount of reinforcement) of gentle slopes is very sensitive to the reinforcement length. A small reduction in the reinforcement length (for instance, from L/H = 0.46 to 0.45) would, in this case, produce a significant drop in the critical height calculated from the mechanism associated with the reinforcement pull-out (down to $\gamma H/k_t$ = 32.81), whereas the critical height calculated from the rupture regime (surface A) remains independent of whether the length of reinforcement L/H is 0.45 or larger.

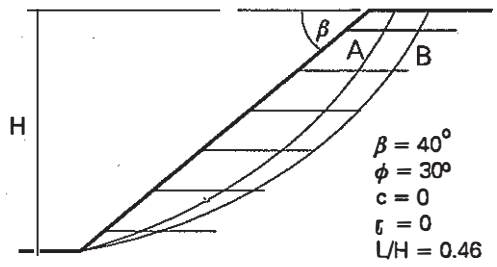

Fig. 4. Critical failure surfaces for a 40-degree slope

The latter example shows clearly how sensitive the slope safety can be to the reinforcement length. Simplifications in calculations of required reinforcement length, therefore, have to be used with caution.

7 CONCLUDING REMARKS

The kinematical approach of limit analysis was shown to be an effective method for stability calculations of reinforced slopes. Calculations were restricted to the rotational mode of failure. Examples were shown where an upper bound to the critical slope height ($\gamma H/k_t$) was calculated for a slope with a given average reinforcement strength (k_t). Alternatively, the results can be presented as a lower bound to the required reinforcement strength ($k_t/\gamma H$) for a slope of a given height.

It is very important that the geometry of failure mechanisms be optimized, subject to constraints imposed by the kinematical admissibility, to arrive at the best bound to the critical height or the required amount of reinforcement for the structure. An optimization procedure revealed that, in slopes with pore water pressure, the top layers of reinforcement may be subjected to compression, leading to kinking, and, thus, eliminating their contribution to stability. Unexpected circumstances arise also for gentle slopes, where the reinforcement layers which undergo pull-out, or are by-passed by the failure surface altogether, are the ones in the middle of the slope rather than those at the top.

Acknowledgements

The work presented in this paper was sponsored by the National Science Foundation, grant No. CMS9301494. This support is greatly appreciated.

REFERENCES

Jewell, R.A. (1990). "Revised design charts for steep reinforced slopes." in: *Reinforced Embankments, Theory and Practice*, Thomas Telford, London, 1-30.

Leshchinsky, D. and Boedecker, R.H. (1989). Geosynthetic reinforced soil structures. ASCE J. Geot. Eng., 115(10), 1459-1478.

Michalowski, R.L. (1994). Limit analysis of slopes subjected to pore pressure, in 8th. int. Conf. on Computer Methods and Advances in Geomechanics, Morgantown 1994, vol. 3, 2477-2482.